Methods for Cavitation Prediction on Tip-Modified Propellers in Ship Wake Fields

Shin, Keun Woo; Regener, Pelle Bo; Andersen, Poul

Published in:
Fourth International Symposium on Marine Propulsors

Publication date:
2015

Document Version
Publisher's PDF, also known as Version of record

Fourth International Symposium on Marine Propulsors
smp'15, Austin, Texas, USA, June 2015

Methods for Cavitation Prediction on Tip-Modified Propellers in Ship Wake Fields

Keun Woo Shin[1], Pelle Bo Regener[2], Poul Andersen[2]

[1] Propeller & Aftship R&D Department, MAN Diesel & Turbo, Frederikshavn, Denmark
[2] Department of Mechanical Engineering, Technical University of Denmark (DTU), Kgs.Lyngby, Denmark

ABSTRACT

Unsteady cavitation simulations on a tip-modified propeller in behind-hull condition are made by both Boundary Element Method (BEM) and Computational Fluid Dynamics (CFD).

As the hull geometry typically is not disclosed to the propeller designer and thus cannot be included in the simulation, other measures must be taken to account for the ship's wake field. In CFD, different wake models using a non-uniform inlet flow and momentum sources are tested to achieve resulting axial and transverse flows in the propeller plane that resemble the desired wake field.

Also, the simulations are carried out with two types of hull wake fields: One originating from model test measurements and the other from a bare hull RANS simulation at the cavitation test Reynolds number. By comparing simulation results, the different numerical approaches are evaluated for accuracy of the unsteady cavitation prediction as a propeller design tool complementing the cavitation tunnel test.

Keywords

Cavitation, Unconventional propeller, CFD, BEM, Hull wake, DES

1 INTRODUCTION

Up-to-date marine propellers are designed to perform with a certain extent of cavitation for optimum propulsive efficiency, but excessive extent and certain types of cavitation have the risk of high hull pressure pulses, blade surface erosion and thrust breakdown. Propeller cavitation becomes particularly unsteady and complex due to the interaction of the propeller flow and the non-uniform wake field behind the hull.

Potential flow-based techniques, such as the boundary element method (BEM), have limitations in accounting for turbulent viscous flows and corresponding aspects of cavitation phenomena, but are still a practical tool for cavitation estimation in the propeller design phase and are used on a regular basis. As the computational capacity increases, fully viscous and non-linear CFD methods also become more practical in marine applications. Unsteady cavitation simulations on a propeller with a hull model or with a hull wake flow by RANS, DES and LES have been validated against cavitation tunnel test results (Bensow & Bark 2010, Boorsma & Whitworth 2011, Paik et al. 2013, Shin 2014). RANS cavitation simulations show overall agreement in sheet cavitation variations, but unstable sheet cavitation, detached sheet cavitation and tip vortex cavitation are not reproduced well by RANS. LES and DES show higher accuracy in simulating these more complex types, but LES and DES require more computational effort than RANS.

The interest in improving propulsive efficiency is increasing with high fuel price and environmental concern. Several kinds of tip-modified propellers have been introduced to reduce energy loss from tip vortices (Andersen et al. 2005). The blade geometry is more complicated due to tip bending and the variation of sheet cavitation and tip vortex cavitation is different from conventional propellers. Since the lifting surface of the tip-modified blade is not on cylindrical planes and the three-dimensional propeller flow is more pronounced, typical implementations of potential flow-based methods, which are a common tool for blade design and analysis, have limitations in estimating cavitation. The simulations in the following sections deal with Kappel propellers that feature a smooth tip bending towards the suction side.

Unsteady cavitation simulations on tip-modified propellers are made by both BEM and CFD. In CFD, detached eddy simulation (DES) is used to estimate detached cavitation with higher accuracy than RANS. Still, DES requires less computational effort than large eddy simulation (LES). The accuracy in simulating unsteady sheet cavitation, detached cavitation and tip vortex cavitation is evaluated. The computational effort is also considered in order to routinely use the numerical analysis on the propeller design.

Instead of modeling the hull, the velocities from a wake measurement are typically applied to numerical analyses as inflow, as it is common practice that hull wake measurements are provided to propeller designers, while

hull lines are not made available. It is also advantageous in terms of computational effort to exclude the hull. While hull wake fields are measured at model-scale and a ship speed scaled by Froude's law in towing tanks, cavitation tunnel tests are made at a high Reynolds number by increasing the tunnel flow speed and propeller revolutions. The propeller speed in a cavitation tunnel is typically 3-5 times higher than in a towing tank. As the boundary layer is thinner at higher Reynolds numbers, the high wake region is more compact in the cavitation tunnel test.

As the hull geometry is available in this particular case, a bare hull RANS simulation is made at the flow velocity from the cavitation tunnel test to obtain the nominal wake field at the comparable Reynolds number. Both, the hull wake field from the towing tank measurement and from the RANS simulation are applied to cavitation simulations in CFD and BEM to highlight the impact of the wake field.

All three velocity components of the wake field can be applied directly to the blade surface in the panel code (BEM), whereas this is not possible in CFD. Here, the inlet boundary is located three propeller diameters upstream of the propeller plane. When all three velocity components of the non-uniform wake field are applied to the domain inlet boundary, the inflow becomes chaotic on the way to the propeller plane and is unlikely to represent the hull wake properly. Therefore, measures must be taken to achieve a realistic inflow to the propeller in CFD. Only the non-uniform axial wake component is applied at the domain inlet, which then can be combined with an additional inlet flow or momentum sources to generate a sensible transverse wake flow. Three different arrangements of this approach are tested in a simple fluid domain without a propeller.

2 BARE HULL SIMULATION

Bare hull simulations are made by a RANS solver with k-ω SST turbulence model and high-y^+ wall treatment. For validation purposes, both the flow corresponding to the resistance test and the cavitation test are simulated. When applicable, the free surface is captured by a multiphase flow model based on the Volume of Fluid (VOF) approach. High-resolution interface capturing (HRIC) is used for the definition of a sharp free surface without excessive smearing. The ship position is fixed to represent the sinkage and trim from the towing-tank resistance test. All CFD simulations are made using the commercial CFD solver StarCCM+.

Unsteady simulations are made with a second-order implicit time advance scheme, a time step of Δt=0.02s and 5 inner iterations. The convection term is discretized by a second-order upwind scheme. The discretization of the diffusion term is based on gradients of the element shape functions.

Since our simulations are aimed at the validation against the model test, all computations are made in model scale. The model-scale ship waterline length is L_{WL}=7.6m. Only the port-side half of the hull is modeled in a rectangular domain with distances of $1.5L_{WL}$ upstream and above the hull and $2.5L_{WL}$ downstream and below. The first cell height is Δh≈1mm and the hull surface grid size is Δh≈1-3mm, which results mostly in y^+≤4. Six prism layers are applied to the hull surface. The hexahedral volume mesh is trimmed by the hull geometry.

Bare hull simulations are made at two ship speeds of V_S=1.5m/s and 4.5m/s. V_S=1.5m/s is the towing tank carriage speed in the wake measurement, which corresponds to the service Froude number. V_S=4.5m/s is the cavitation tunnel flow speed. The propeller speed is accordingly increased to N=24.0rps to reach the thrust coefficient K_T obtained in the towing-tank self-propulsion test, whereas N=7.8rps in the self-propulsion test.

Simulations are run for longer than 90s corresponding to 4,500 time-steps. The computed resistance at V_S=1.5m/s is overpredicted by 3.9%. The mean value of the maximum and minimum in the last 200 time-steps is taken as the final result.

To extract the wake field, velocities are extracted at points corresponding to the towing tank wake measurement. The probe points shown in Fig. 1 lie on six radii in the propeller plane with an angular resolution of 5 °.

As can be seen from Fig. 2b, the axial and transverse velocity components from the simulation at V_S=1.5m/s show good agreement with the wake measurement (Fig. 2a) at outer radii of r/R>0.5. But the simulation results in higher axial wake fraction and weaker radial flow at inner radii compared to the experiment as the bilge vortex is underpredicted.

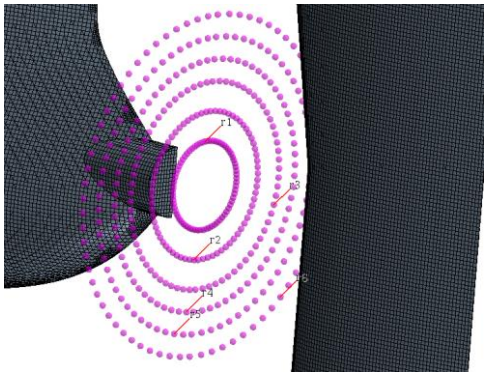

Figure 1: Velocity probe points in the propeller plane

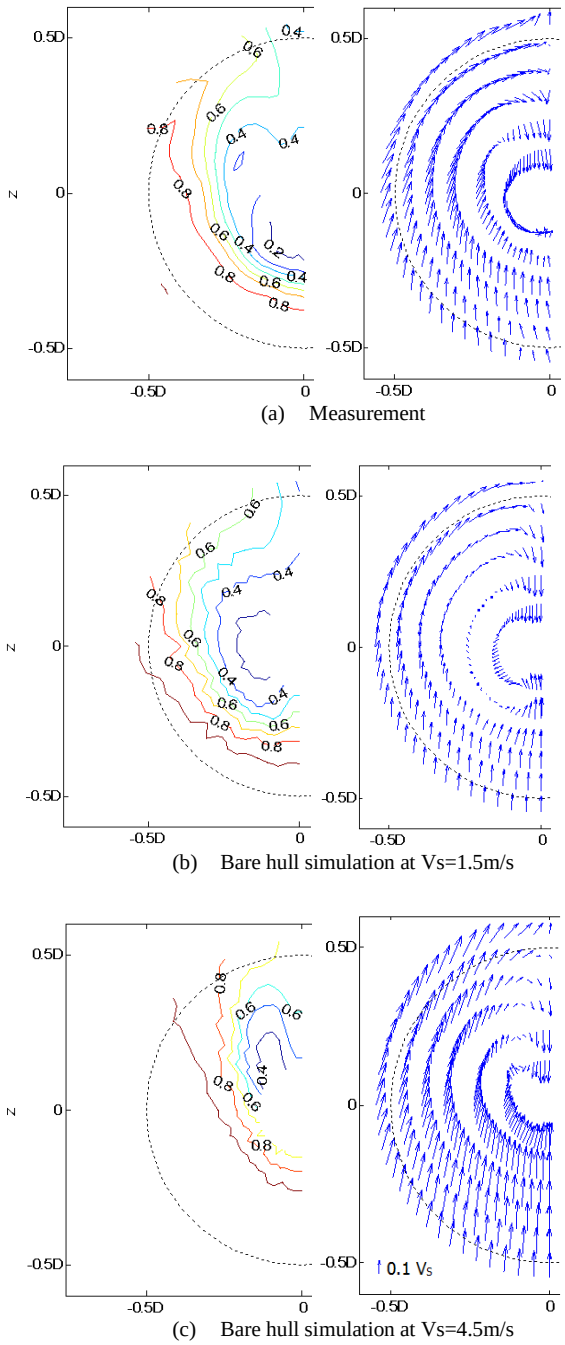

(a) Measurement

(b) Bare hull simulation at Vs=1.5m/s

(c) Bare hull simulation at Vs=4.5m/s

Figure 2: Axial (left) and transverse (right) velocity components of the hull wake field from a measurement and bare hull simulations

The simulation at the cavitation tunnel speed shows a more contracted wake field due to the higher Reynolds number and it can also be seen that the axial wake peak at the 12 o'clock position becomes less pronounced with the bilge vortex moving up in position. The upward transverse wake becomes stronger.

3 WAKE MODELING

As the ship's wake field cannot be applied directly to the propeller plane in CFD simulations, three wake models are set up to reproduce a given wake field in the middle of the domain. For testing purposes, cases are run that resemble the grid for cavitation simulations, excluding the actual propeller. The computational setup with a rudder and a shaft (See Fig. 3) is the same in terms of domain size and mesh condition. As shown in Fig. 5, the velocity field is probed in the same fashion as in the bare hull simulations.

Three types of wake models are to be tested. Model 1 only uses the axial component of the non-uniform wake field as inflow boundary condition. Model 2 is a combination of this non-uniform axial inlet wake and momentum sources located halfway between the inlet and the propeller plane inducing radial and tangential velocities. In Model 3, the uniform transverse inlet flow shown in Fig. 6 is added to the setup of Model 2.

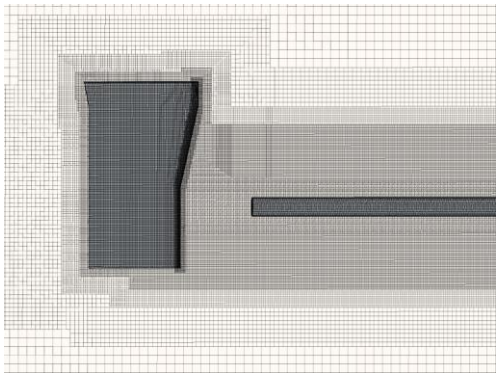

Figure 3: Volume mesh on a longitudinal section for wake simulations without a propeller flow

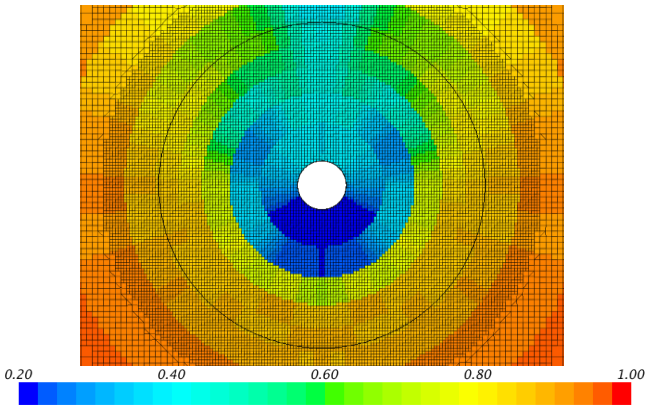

Figure 4: Non-uniform axial inlet flow velocity V_X/V_S

The non-uniform axial wake that is part of all three models is applied directly at the inlet boundary, which is located three propeller diameters upstream of the propeller plane. This distance between the inlet and propeller plane is required to avoid numerical instability due to upstream perturbation of the propeller. Fig. 4 shows the axial wake

component mapped to the inlet mesh without smoothing. The axial flow distribution becomes smooth on the way to the propeller plane.

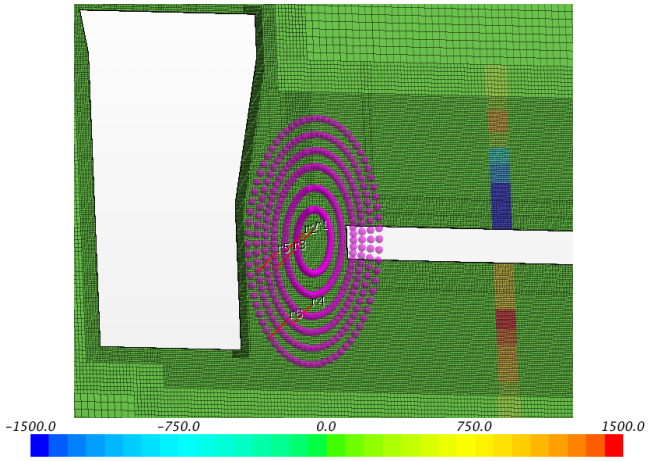

Figure 5: *z*-direction momentum source in N/m^3

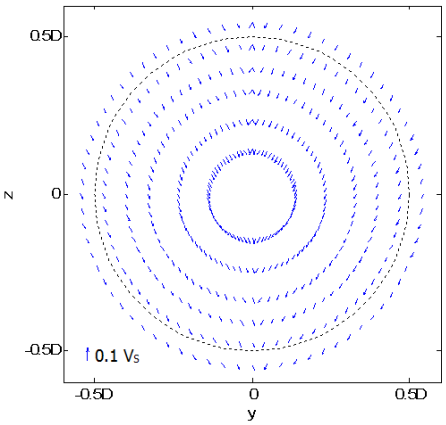

Figure 6: Transverse inlet flow

When applying Model 1 that only uses the axial inlet flow, the simulation result shows that the axial flow distribution at the propeller plane (See Fig. 7a) agrees well with the initial axial inflow at the inlet i.e. the axial component of the wake measurement as shown in Fig. 3a. There are no considerable transversal velocity components in the propeller plane.

In Model 2, the transverse wake flow is formed using momentum sources. The local *y*- and *z*-direction momentum source strengths are found from a linear relationship to the transversal velocities.

Although there are formulas based on the Rankine-Froude momentum theory to estimate source-term strength according to a local wake flow, the multiplying factor is calibrated iteratively by numerical tests, because it is hard to control the number and size of cells under the influence of the momentum source in an unstructured grid.

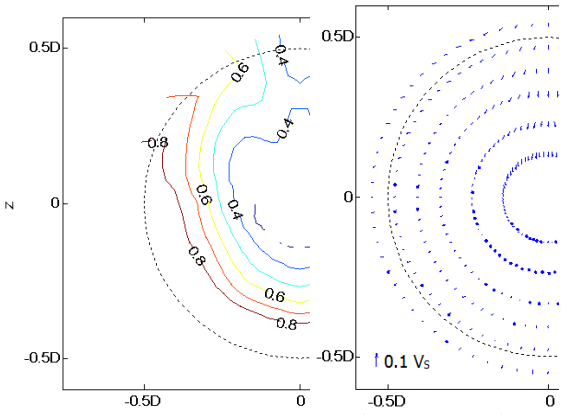

(a) Model 1: Non-uniform axial inlet flow

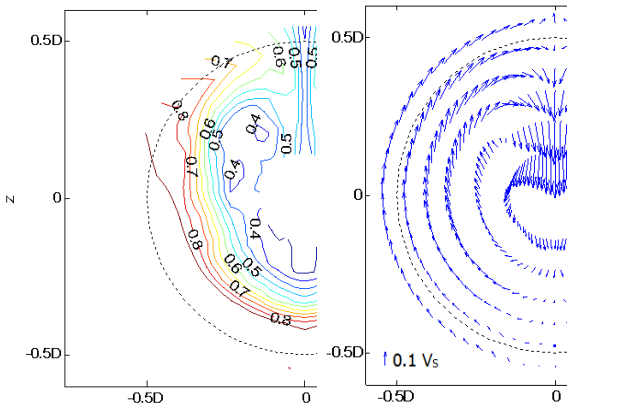

(b) Model 2: Non-uniform axial inlet flow + momentum source

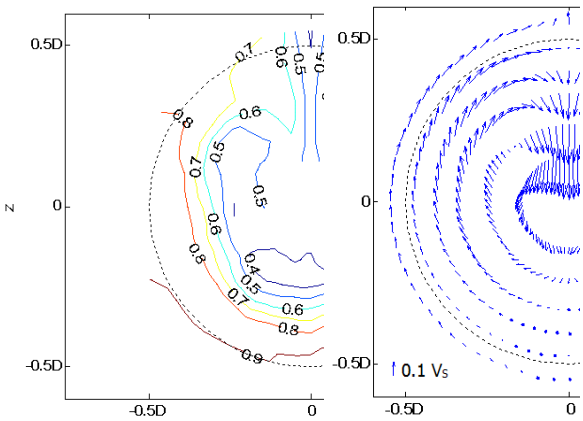

(c) Model 3:
Non-uniform axial inlet flow + momentum source + transverse inlet flow

Figure 7: Axial (left) and transverse (right) velocity components at the expected position of the propeller plane from wake simulations with three wake models

Momentum sources are applied one propeller diameter upstream of the propeller plane. Fig. 5 shows the z-direction momentum source on a longitudinal section.

The velocity field in the propeller plane using Model 2, which consists of a non-uniform axial inlet flow and

momentum sources, shows a characteristic bilge vortex in the upper half of the propeller disk (Fig. 7b). But the upward flow is not reproduced well in the lower half and the high axial wake region has a larger vertical extent compared to the measurement.

When momentum sources are modified locally as an effort to adjust the wake flow, the overall wake becomes disorganized with disturbing an underlying equilibrium. Hence a transverse inlet flow with uniform downward and inward components (towards the centerline, see Fig. 6) is added. The direction and magnitude of the transverse inlet flow are adjusted to improve the general agreement with the measured wake in the propeller plane. The average velocity magnitude of the transverse inlet flow is about 5 times smaller than the measurement.

Running the test case with Model 3, consisting of this additional inlet flow and the elements of Model 2, the axial wake distribution in Fig. 7c becomes slighter closer to the measurement and the strong downward flow is weakened at inner radii of the upright blade position, compared to the case with Model 2. The following CFD cavitation simulations use Model 3 to apply the wake fields.

4 CAVITATION SIMULATION

A 4-bladed Kappel propeller with a model-scale diameter of 250 mm serves as test case for cavitation simulations. It has been selected as it is a propeller with a low area ratio of Ae/Ao=0.38 and shows a large extent of sheet cavitation. The sheet is characterized by an uneven surface and detaches close to the leading edge. Cloud cavitation can be observed at blade angles 30-50 °. The reference cavitation tunnel test has been conducted with a complete ship model at SSPA.

A condition of V_S=4.5m/s, N=24.0rps and σ_N=3.8 is considered, where σ_N is the cavitation number with ND as a reference velocity. In cavitation tunnel tests, N is adjusted with keeping a tunnel flow speed constant to reach K_T from a towing-tank self-propulsion test. In simulations, V_S and N from the cavitation test are used and the wake fraction w of the axial inlet flow is adjusted to reach K_T from the model test.

4.1 BEM cavitation simulation

Representing a simple but proven tool that is still used at several stages of propeller design, a basic implementation of the boundary element method (BEM) is used for cavitation estimation. It uses quadrilateral panels on the propeller blades and blade wake and does not include the propeller hub. The blade wake is rigid and as there is no cavitation model, cavitation is defined as the area where the blade surface pressure falls below the local vapor pressure.

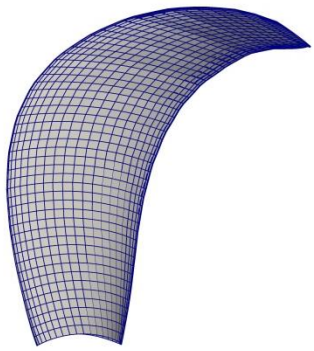

Figure 8: BEM blade mesh

Each blade is discretized with 50 uniformly distributed panels in spanwise direction and 22 panels per side chordwise. As is apparent from Fig. 8, a cosine distribution is used in chordwise direction. Simulations are carried out in model scale and all environmental conditions are set to reproduce the conditions in the cavitation tunnel.

Figure 9 shows the cavitation pattern (according to above simplified definition) at blade angles 340-60 ° for the measured wake distribution. Comparing the chordwise cavitation extent with the experimental results shown in Fig. 11, it is obvious that the BEM underestimates this fairly extensive and possibly even erosive cavitation.

With regard to chordwise extent, no considerable differences can be observed between simulations using the measured and the simulated wake field after adjusting w for K_T.

Both the radial extent and the angular range of cavitation (range of blade positions), however, are predicted with fair accuracy.

Figure 9: Cavitation pattern as predicted by BEM (Blade angles 340-90 °, corresponding to Fig. 11)

4.2 CFD cavitation simulation

CFD cavitation simulations are made by Detached Eddy Simulation (DES) with the *k-ω* SST turbulence model. Unsteady computations are performed with a time step corresponding to 5 ° propeller rotation for the first five revolutions. The time step size is reduced to a value corresponding to 1 ° propeller rotation afterwards and the simulation is continued for five additional revolutions. The rotation of the propeller is simulated as rigid body motion with a sliding mesh.

The built-in cavitation model in StarCCM+ is used. It is an Eulerian multiphase model employing of the Volume-of-Fluid (VOF) approach and a vapor transport equation based on the Rayleigh-Plesset equation. The gravity force is applied with the shaft depth as a reference altitude.

In Fig. 10, a grid size of Δx=0.5-1.0mm is applied to the surface mesh of blade, hub and rudder. Blade edges have a finer grid of Δx=0.12-0.5mm. Six prism layers with Δh=0.12-0.25mm are on all wall surfaces, which results mostly in $y^+ \leq 2$. A fine volume mesh of $\Delta x \approx$0.5mm is along blade tips and expected tip vortex trails.

Figure 10: Computational mesh for cavitation simulations

In Fig. 11, cavitation variations from CFD are compared with that from a cavitation tunnel test. An isosurface of 10% vapor fraction is taken as a cavitation interface. Using a 50% vapor fraction interface gives a similar distribution as a 10% interface in a sheet cavitation region, but the 50% interface does not capture the detached cavities.

In both experiment and CFD, sheet cavitation starts appearing at a blade position of about 330-340 ° and disappears at 90-100 °, where 0 ° corresponds to 12 o'clock. There is almost no cavitation in the lower half of the propeller disk due to lower hull wake and higher hydrostatic pressure.

Sheet cavitation grows from 340 ° to 30 °. While the simulation with the measured wake shows less chordwise extent of sheet cavitation than the experiment at 0 °, the other simulation with the simulated wake overestimates the radial extent. At 20-60 °, both simulations have a good agreement in the starting radius of sheet cavitation with the experiment. The simulation with the measured wake underestimates the chordwise extent of sheet cavitation, but the other simulation shows a good agreement in the chordwise extent.

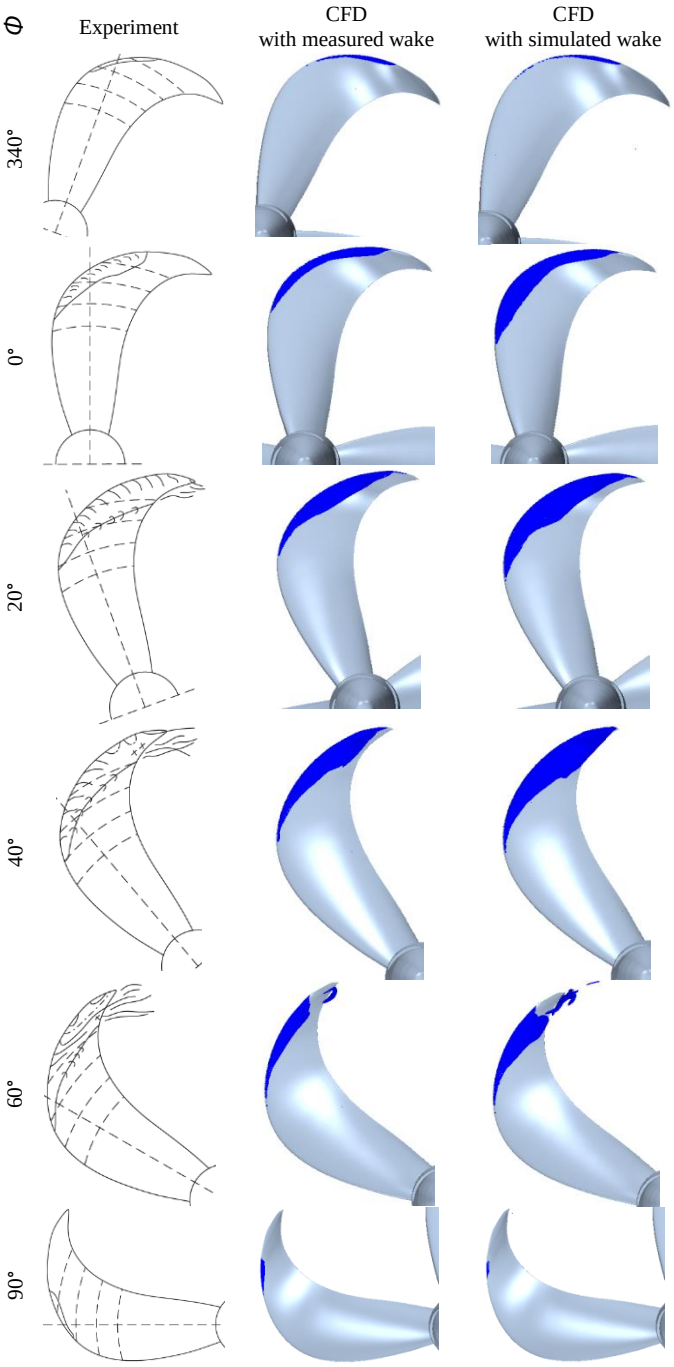

Figure 11: Unsteady cavitation at different blade angles from a cavitation tunnel test and CFD simulations

While the experiment shows detached cloud cavitation at 20-60 °, both simulations show detached cavitation at 50-60 ° and the extent is smaller than the experiment. It may be because microscopic scales of fine cloud cavitation are less

than the volume mesh size of $\Delta x \approx 0.5$mm and only relatively large-scale structures of cloud cavitation are reproduced by CFD.

The simulation with a simulated wake shows a slightly larger extent of sheet cavitation, because the high wake region of the simulated wake is more concentrated along the upright blade position than the measured wake, whereas the high wake region is widely distributed around inner radii in the measurement. The extent of cloud cavitation is also a bit larger in the simulation with a simulated wake than the other simulation, even though both show less cloud cavitation than the experiment.

5 CONCLUSION

Performing realistic cavitation simulations in CFD requires a technique to reproduce a given wake field in the propeller plane. This aspect gains importance in design situations where the hull form is unknown. Wake models that combine non-uniform inflow and momentum sources seem to be able to satisfy this basic requirement, even though the presented method involves considerable manual work on a case-by-case basis. Both, the axial wake distribution and the characteristic bilge vortex are generated in the propeller plane, showing good agreement with the wake measurement. The wake model is applied to cavitation simulations instead of including a hull model.

The intriguing simplicity of use, including the easy application of given wake fields and very low computational effort are major advantages of boundary element methods over more powerful field methods. The BEM results suggest that the panel method is suitable for preliminary cavitation checks in the design phase as the radial extent and the angular range of cavitation occurrence are predicted with acceptable accuracy. However, implementations without a cavitation model fail to predict the chordwise extent by a large margin. In the case at hand, there is no indication of the tendency to erosive behavior. More complex types of cavitation, such as cloud cavitation, are unlikely to be captured anyhow. Therefore, a more advanced method is required for these cases. The agreement of the DES simulations and the cavitation tunnel observations indicates that DES can be an appropriate tool to also predict fairly complex cavitation phenomena on tip-modified propellers.

The comparison with experimental results shows that the simulation with the high-Re wake has higher accuracy in estimating extents of sheet and cloud cavitation than simulations using the measured nominal wake field, which reinforces the notion that hull lines availability is of high importance to the propeller designer as well.

REFERENCES

Andersen, P., Friesch, J., Kappel, J.J., Lundegaard, L., and Patience, G., (2005), "Development of a marine propeller with nonplanar lifting surfaces," Marine Technology, Vol. 42, No. 3

Bensow, R. E., and Bark, G., (2010), "Simulating cavitating flows with LES in Openfoam," ECCOMAS CFD, Lisbon, Portugal

Boorsma, A. and Whitworth, S., (2011), "Understanding details of cavitation," SMP'11, Hamburg, Germany

ITTC, (2011), "ITTC- Recommended procedures and guidelines: Nominal wake measurement by a 5-hole pitot tube," 26th ITTC

Menter, F. R., and Kuntz, M., (2003), "Adaptation of eddy-viscosity turbulence models to unsteady separated flow behind vehicles," Pro. Conf. The Aerodynamics of Heavy Vehicles: Trucks, Busses and Trains, Asilomar, CA, Springer

Paik, K., Park, H., Seo, J., (2013), "URANS simulations of cavitation and hull pressure fluctuation for marine propeller with hull interaction," SMP'13, Tasmania, Australia

Shin, K.W., (2014), "Cavitation simulation on Kappel propeller with a hull wake field", NuTTS2014, Marstrand, Sweden